



A method to determine the correct photocatalyst concentration for photooxidation reactions conducted in continuous flow reactors

Clemens R. Horn* and Sylvain Gremetz

Letter

Open Access

Address:
Corning European Technology Center, 7 Bis Avenue de Valvins,
F-77215 Avon Cedex, France

Email:
Clemens R. Horn* - Clemens.R.Horn@gmail.com

* Corresponding author

Keywords:
catalyst concentration; channel height; flow chemistry; photooxidation

Beilstein J. Org. Chem. **2020**, *16*, 871–879.
doi:10.3762/bjoc.16.78

Received: 26 February 2020
Accepted: 16 April 2020
Published: 27 April 2020

This article is part of the thematic issue "Advances in photoredox catalysis".

Guest Editor: T. Noël

© 2020 Horn and Gremetz; licensee Beilstein-Institut.
License and terms: see end of document.

Abstract

When conducting a photooxidation reaction, the key question is what is the best amount of photocatalyst to be used in the reaction? This work demonstrates a fast and simple method to calculate a reliable concentration of the photocatalyst that will ensure an efficient reaction. The determination is based on shifting the calculation away from the concentration of the compound to be oxidized to utilizing the limitations on the total light dose that can be delivered to the catalyst. These limitations are defined by the photoflow setup, specifically the channel height and the emission peak of the light source. This method was tested and shown to work well for three catalysts with different absorption properties through using LEDs with emission maxima close to the absorption maximum of each catalyst.

Introduction

The renaissance of photochemistry that occurred over the last decade has been described as “old light through new windows”, and much of this work centered on the combination of light with continuous flow reactors [1-6]. The reason for this increased interest is that continuous flow photochemical reactors can overcome various limitations that occur when the same reaction run in batch reactors [7]. For example, the flow reactor can overcome the difficulties that occur upon scale-up. The

most desirable approach for industrial-scale reactions is described by the quote “the best approach to the scale-up of a photoreaction seems to be the enlarging of a laboratory-type prototype reactor, with the important parameters being changed as little as possible” [8]. This phrase describes the approach used to scale up flow reactors to an industrial scale [9,10]. This is particularly true when it comes to biphasic reactions, like a gas/liquid reaction as is the case for photooxidations [11]. An inter-

esting aspect of photooxidations is that the combination of light, the “greenest reagent” oxygen, and a catalyst as well as applying mild process conditions under process-intensified conditions can be considered a very sustainable setup [12–14].

The scaling-up of photoflow reactors has also been affected by the increased use of LED sources over mercury arcs and other light sources commonly used in industry and classical synthetic organic photochemistry. LEDs typically have much narrower emission spectra when compared to these light sources, all of which have broad emission spectra except for low-pressure sodium vapor lamps [15,16]. These broad emission spectra pose some further complications as they are ultimately a rather inefficient way to use the energy and provide wavelengths that can effectively increase the risk of side reactions [17]. The fact that only a portion of the emitted light is used in the reaction can further complicate the scale-up of the light source and design of the reactor. LED sources have continuously been evolving and will continue to do so because when being employed, the light source is no longer a limiting factor in the design of a larger-scale photoreactor setup [18]. Since an LED provides a narrower emission wavelength, the appropriate wavelength above 365 nm can be selected for every reaction, and the scale-up can be achieved by simply increasing the number of the LEDs applied [19]. The narrower spectra, while providing many benefits and likely reducing the occurrence of side reactions, also facilitate that other factors become more important. Notably, an exact description of the photoflow setup is now crucial to ensure reproducible experiments [20,21].

Results and Discussion

The effect of 1 mol % photocatalyst

This work was accomplished using the Corning® Advanced-Flow™ Lab Photo Reactor, providing a robust platform for a

rapid screening of the reaction conditions (e.g., the wavelength) and, for photooxidation reactions, the catalysts. For a schematic reaction setup see Figure 1, and further details can be found in Supporting Information File 1 [22]. As a test reaction, we rapidly screened 9 photocatalysts for the oxidation of citronellol (Scheme 1), using the conditions described by Lévesque and Seeberger [23].

The reaction conditions used for the experiments shown in Scheme 1 are detailed in Figure 2 below, and the best results are highlighted in grey.

The conversions of the photooxidation reactions were determined under similar reaction conditions using 11 different wavelengths (10 sources with defined wavelength and 1 white light source with a color temperature of 4000 K). At the same time, the transmission spectra of all starting solutions were recorded using a cuvette with a path length of 0.5 mm, which is close to that of the fluidic module in the reactor (0.4 mm). The lower-right value in each field of Figure 2 corresponds to the transmission recorded at the LED emission maximum. In about 30% of the tests, a complete conversion was obtained (highlighted in grey in Figure 2), but only in 15% of the cases, the catalyst concentration was high enough to absorb all the light at the given wavelength (highlighted with a bold frame, transmission < 1%).

Overall, the results show that 1 mol % of the catalyst was not the ideal concentration for the various initiators. For example, in the extreme case of using tetraphenylporphyrin (TPP, **H**), the concentration was so high that a complete conversion was obtained at any wavelength. This included a case where the reaction was performed at 624 nm, with the measured transmission for the solution being 100% (Figure 3). There was still enough

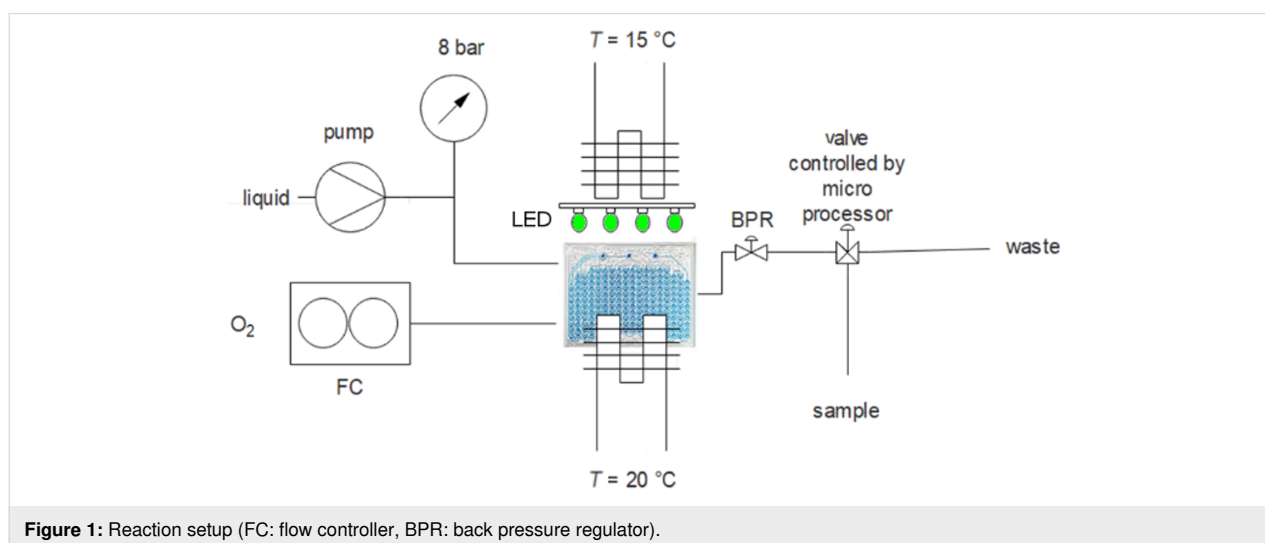
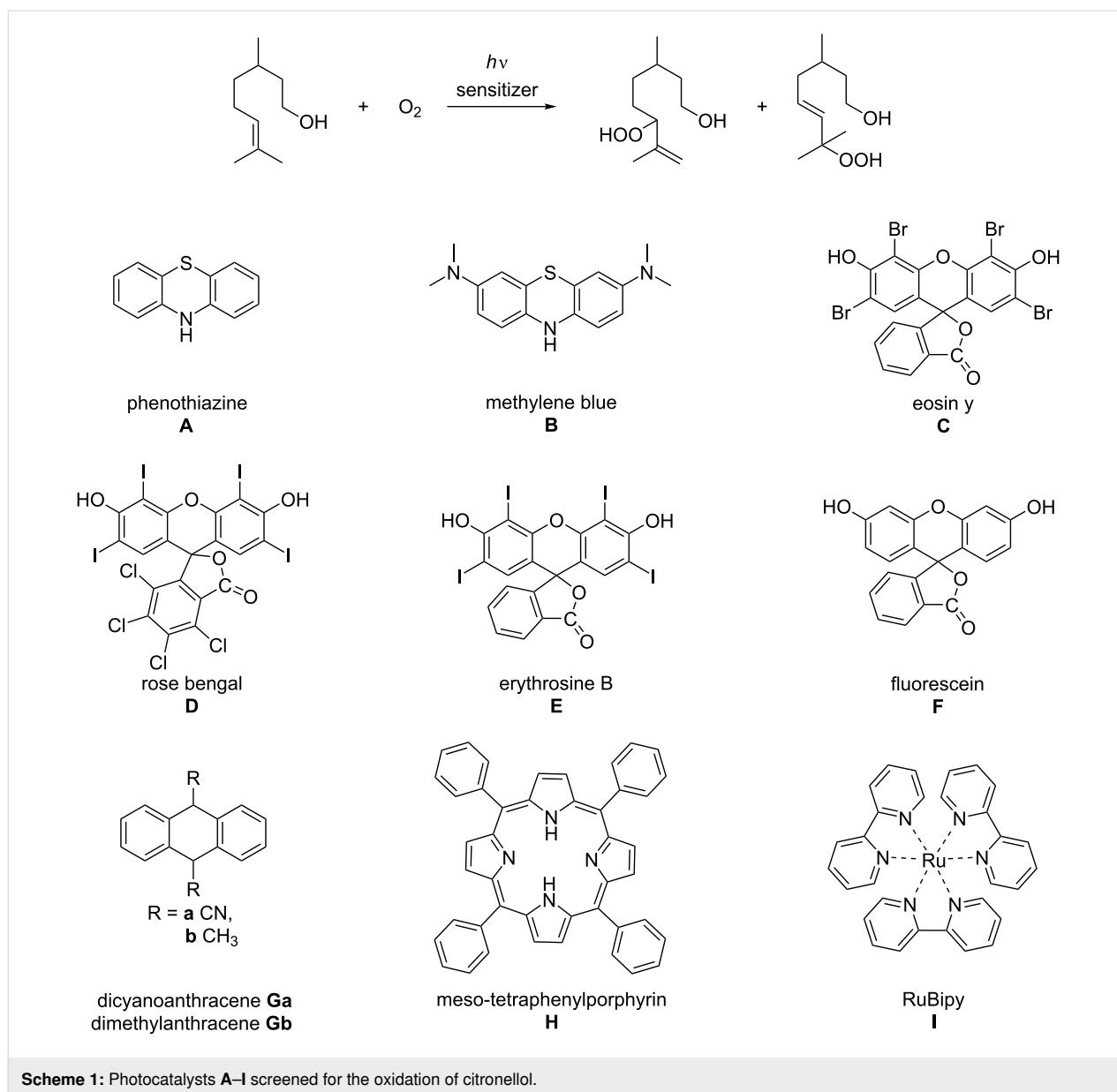


Figure 1: Reaction setup (FC: flow controller, BPR: back pressure regulator).



overlap with the Q bands of **H** at 593 and 649 nm to provide a high enough light intensity for the reaction, and thus causing the complete conversion.

A method to obtain an estimation of the required photocatalyst

As the photooxidation reaction has been shown to be dependent on the photocatalyst concentration, a simple method to determine the required amount in a reaction mixture is necessary. Further, when considering an industrial process, the concentration of the photocatalyst will have not only an economic impact but could also impact the downstream process or subsequent synthetic steps. It may be noted that in typical studies on photooxidation reactions, the concentration of the reactants is

usually varied, while the catalyst concentration is rarely addressed [24–26].

To study the required photocatalyst concentration, we pursued a different approach based on the realization that in a photochemical reaction, the often overlooked key reagent is, in fact, the light, and through the subsequent interaction between light and the photocatalyst, the light is transformed. Following this logic led to the observation that one needs to more carefully consider not only the concentration of the catalyst but the details of how and to what extent the light interacts with the catalyst in the region where it is exposed to the light. A good starting point for this analysis was the Bunsen–Roscoe law of reciprocity, which states that a photochemical effect is directly proportional to the

Conv ^a Trans ^b	365	375	383	396	407	424	443	467	524	624	4000k
A	2 71	3 88	2 99	1 100	1 100	0 100	1 100	0 100	0 100	0 100	0 n.a.
B	33 49	53 53	46 53	59 64	28 96	30 100	63 93	66 61	65 29	>96 0	85 n.a.
C	62 45	81 39	84 37	>96 37	89 45	>96 68	88 35	62 20	55 26	0 100	36 n.a.
D	92 21	94 46	91 59	>96 59	>96 57	>96 69	>96 62	>96 33	>96 1	4 100	90 n.a.
E	72 29	78 47	80 49	>96 43	93 44	93 72	>96 53	>96 5	95 1	0 100	64 n.a.
F	3 50	8 53	5 57	2 61	9 68	17 91	35 73	35 77	35 94	5 100	26 n.a.
Ga	>96 7	>96 1	>96 3	>96 1	>96 3	>96 1	>96 100	46 100	0 100	0 100	21 n.a.
H	>96 0	>96 0	96 0	>96 0	>96 0	>96 0	>96 28	>96 55	>96 1	>96 100	>96 n.a.
I^c	23 80	26 86	31 92	48 91	49 95	61 100	85 100	59 100	0 100	0 100	12 n.a.

Figure 2: Conversion and transmission at fixed reaction conditions (0.5 N citronellol, 1 mL/min, 1 mol % catalyst, 2 equiv oxygen, 8 bar, 20 °C, reactor volume: 2.7 mL, solvent: ethanol (**B, C, D, E, and F**) or dichloromethane (**A, G, H, and I**)). ^aThe conversion was determined by GC after quenching with PPh₃. ^bTransmission (in %) of the starting solution at 0.5 mm pathlength. ^cCatalyst concentration: 0.1 mol %.

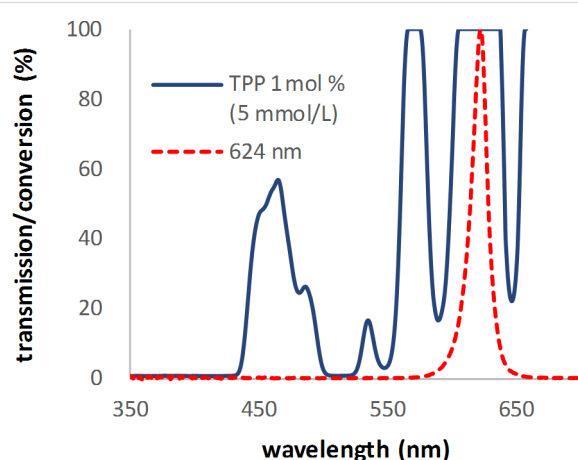


Figure 3: Measured transmission spectrum of a 5 mmol/L (1 mol %) solution of TPP (**H**) in dichloromethane with 0.5 N citronellol and the emission spectrum of the LED with an emission maximum at 624 nm.

total energy dose, which, for a flow reactor, is the product of the light intensity and time [27–29]. The light intensity can be considered as the limiting factor in a flow setup as the space around the reaction channel is limited, as is the power of the light source. The exposure time has less limitations as it is controlled by the flow rate. This implies that in order to conduct an efficient reaction, the use of the light has to be optimized such that the quantity of light reaching the reaction mixture in the channel is large enough to be totally absorbed.

Our approach to considering light more conspicuously as a reagent uses the Bouguer–Lambert–Beer law as a starting point to estimate a concentration close to the optimum. The law in its basic definition is not entirely applicable to a flow reactor but will nevertheless provide a convenient starting point [30,31]. The analysis of the required concentration of the catalyst begins with recognizing how the law is applied and what the differences from the batch approach that it describes are [32]. A flow reactor has a channel height that is a well-defined rectangle, allowing it to be used synonymously to the path length of the light. However, since the path length of the channel is much shorter than the path length used in a classical cuvette measurement, the values obtained from the Beer's law plot may be less accurate. A second contribution to the approximation is that to use all the light, the transmission through the channel needs to be below 1%, which corresponds to an absorption of >2. This condition also limits the use of the Bouguer–Lambert–Beer law since at these high absorption values, the extinction coefficient may exhibit a nonlinear behavior with respect to the concentration of the catalyst [33]. Taking note of the facts above but pressing on and applying Beer's law using a path length fixed at 0.04 cm and an extinction of 2, the molar extinction coefficient still needs to be calculated. Therefore, the molar extinction coefficient needs to be measured separately in a UV–vis spectrometer as the emission maximum of the LED source does, in most cases, not correspond to the absorption maximum of the catalyst. Furthermore, the spectra need to be obtained under the

same conditions under which the reactions take place, i.e., in the same reaction medium, at the same temperature and, if possible, at the same path length. The first two parameters are extremely important as the absorption peak will shift in both height and wavelength depending on the reaction medium and temperature [34]. The path length should be as close as practical to that of the reactor as this will reduce the error imparted by the limitations of the Bouguer–Lambert–Beer law. Table 1 shows the values measured for the extinction coefficient, the LED peak, and the absorption maximum based on the measured values and the predicted concentration for the catalyst using the channel height of 0.04 cm.

Figures 4–6 serve to illustrate three possible examples. For rose bengal (**D**, Figure 4), the emission maximum of the used LED

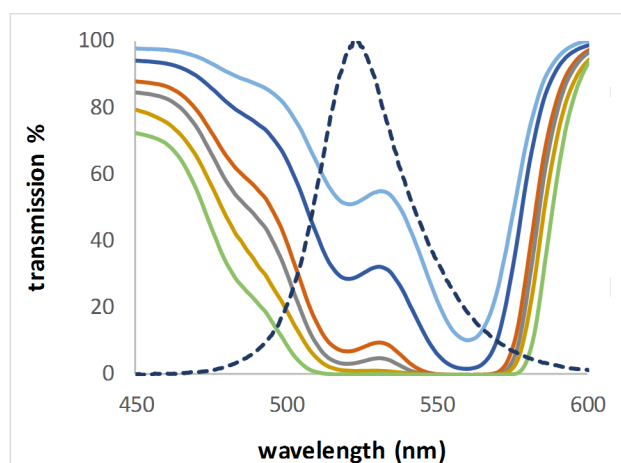


Figure 4: Transmission spectra of rose bengal (**D**) and the emission spectrum of an LED with a maximum at 524 nm (scaled to 100%).

fits nearly to a secondary peak. Dimethylantracene (**DMA**, **Gb**, Figure 5), with three absorption peaks, covers a wide range of possible LEDs. TPP (**H**, Figure 6) is the opposite of **DMA** (**Gb**). It has a very high absorption in a very narrow peak range (that is, a Soret band). As can be seen in Figure 6, the absorption maximum (here transmission 0%) is close to the emission spectra of two of the LEDs, with only 5 and 12 nm difference, respectively. Nevertheless, the calculated concentrations were nearly two or three times higher when compared to the lowest concentration, which would be required for a perfect fit between the absorption maximum and the LED emission. This highlights why it is so important to measure the absorption in the intended reaction medium. A solvent change could shift the maximum by a few nm (TPP: 416 nm in chloroform [37], 418 nm in benzene [38], and 419 nm in toluene [35]).

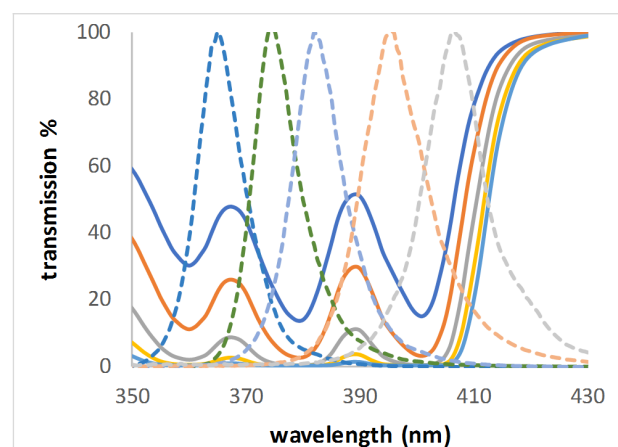


Figure 5: Transmission spectra of dimethylantracene (**Gb**) and emission spectra of LEDs with maxima at 365, 375, 383, 394, and 407 nm, respectively (all scaled to 100%).

Table 1: Measured extinction coefficients and estimated ideal catalyst concentrations.

sensitizer	wavelength [nm]	extinction coefficient [L/(mol·cm)]	literature reference	calculated sensitizer concentration [mmol/L]
rose bengal (D)	560	90000	90400 [35]	0.56
	524 ^a	37400		1.34
	524 ^b	38100		1.31
TPP (H)	424	349000	443000 [35]	0.20
	419	401000		0.12
	407	158000		0.32
DMA (Gb)	407	2800	7500 [36]	17.86
	398	7300		6.85
	396	6000		8.33
	383	6900		7.25
	375	6500		7.69
	365	3800		13.16

Rose bengal (**D**) was measured in ^aethanol or ^bacetonitrile, with 0.5 N citronellol; TPP (**H**) was measured in toluene with 1 N alpha-terpinene; DMA (**Gb**) was measured in toluene with 0.5 N alpha-terpinene.

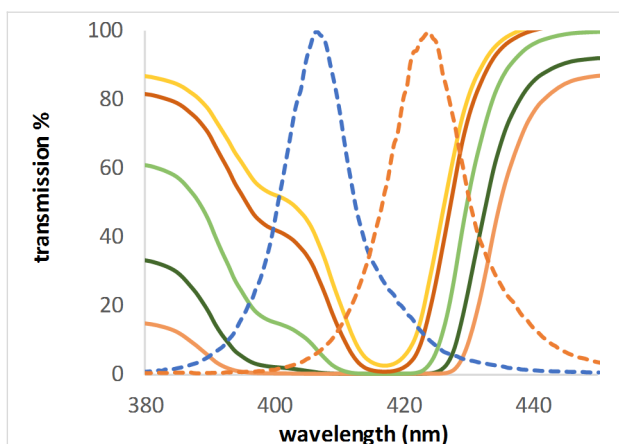
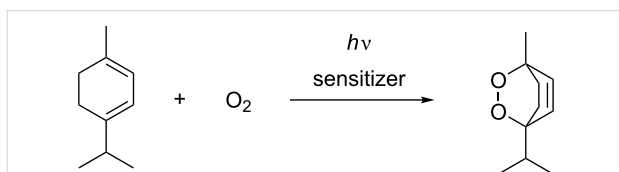


Figure 6: Transmission spectra of TPP (**H**) and emission spectra of LEDs with maxima at 407 and 424 nm, respectively (both scaled to 100%).

Reactions using calculated photocatalyst concentrations

The concentrations calculated for the catalyst were tested using the oxidation of alpha-terpinene (Scheme 2) and the oxidation of citronellol (Scheme 1). All reactions were conducted with 2 equiv of oxygen at 8 bar and 20 °C. The temperature of the light source was kept constant at 15 °C. It is very important to control the temperature of the reaction and the LEDs as the emission and absorption maxima are dependent on the temperature. The (minimum) exposure times were calculated using the liquid flow rate and the flow rate of the gas at the entrance. The results (Figure 7) show that similar results were obtained for the photooxidation of alpha-terpinene using TPP (**H**) at different wavelengths with the corresponding calculated amount of the catalyst.



Scheme 2: Photooxidation of alpha-terpinene.

The reduction of the catalyst concentration to half of the calculated value led to a small decrease in the conversion. This decrease became much larger when the catalyst concentration was further decreased by half again (Figure 8). This exponential decrease can be explained by the fact that the transmission of the light increased exponentially with a decreasing amount of the catalyst.

When DMA (**Gb**) was used and short exposure times were applied, the expected difference in conversion for the wave-

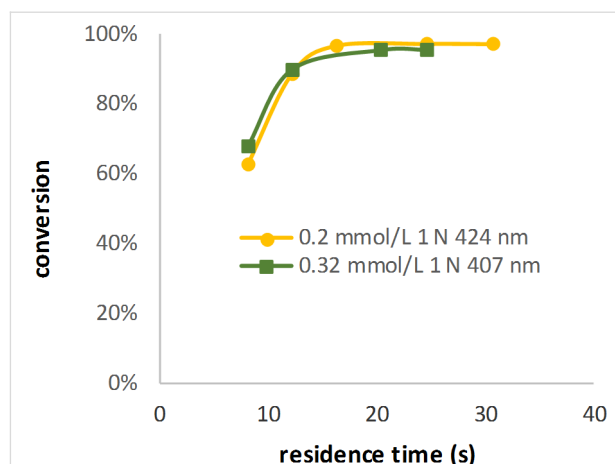


Figure 7: Conversion of alpha-terpinene using the wavelength-adapted TPP (**H**) concentrations.

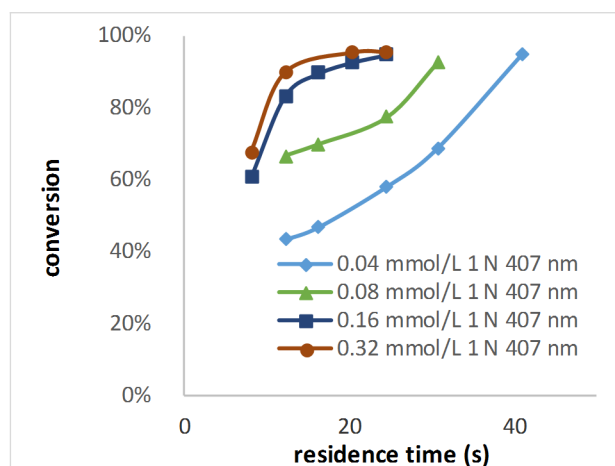


Figure 8: Conversion of alpha-terpinene at different TPP (**H**) concentrations.

lengths 365 nm and 407 nm was seen: the reaction was not complete for any of the used wavelengths (Figure 9). This is completely in line with the observations made for TPP catalyst (**H**) concentrations.

Rose bengal (**D**) gave similar results: increasing the amount of the catalyst by 50% provided a slightly higher conversion for high flow rates, and the change of the solvent from ethanol to acetonitrile had the same impact (Figure 10). This can be attributed to the higher absorption of **D** in acetonitrile [39]. Those two results show the limitation of our approach because if the Bouguer–Lambert–Beer law would have been valid, the conversion should have been the same for the three conditions.

Our approach was to provide a simple means to optimize the catalyst used in conjunction with the maximum amount of light. As such, the question concerning the effect obtained upon varia-

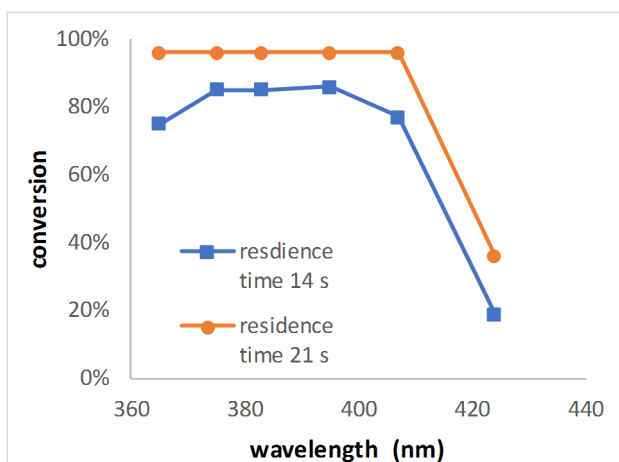


Figure 9: Conversion of alpha-terpinene (0.5 N) as a function of the wavelength using DMA (Gb) as the catalyst (7.25 mmol/L).

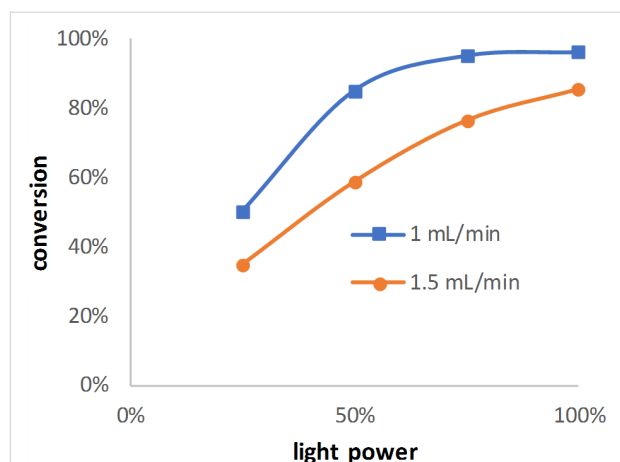


Figure 11: Conversion of citronellol as a function of the light power (0.5 mol/L of citronellol, 1.34 mmol/L rose bengal (D)).

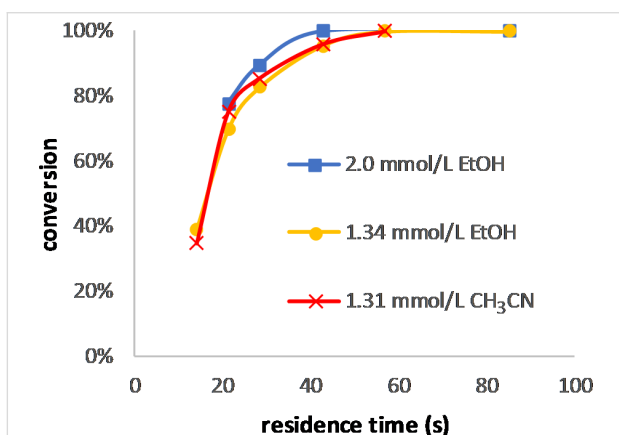


Figure 10: Conversion of citronellol at different concentrations of rose bengal (D).

tion of the light power arose. The answer to this can be found in Figure 11: rather large changes in the conversion of citronellol were observed as a function of the light power, and a greater effect was unsurprisingly observed for the slower flow rate.

The effect of varying the concentration of the reactant concentration of alpha-terpinene while keeping the TPP (H) concentration constant (0.32 mmol/L) is shown in Figure 12.

Here, the ratio of alpha-terpinene to the catalyst decreased from 0.064 mol % to 0.016 mol %, and the conversion increased in a similar manner to that caused by the concentration changes. An exact comparison was not possible as it would be extremely difficult to calculate or even estimate the exact residence time. The residence times in Figure 12 were calculated based on the flow rate of the entrance and exit measurements (the conversion of the oxygen gas was considered). The reduction of the gas caused by the solubility of oxygen at the given pressure in

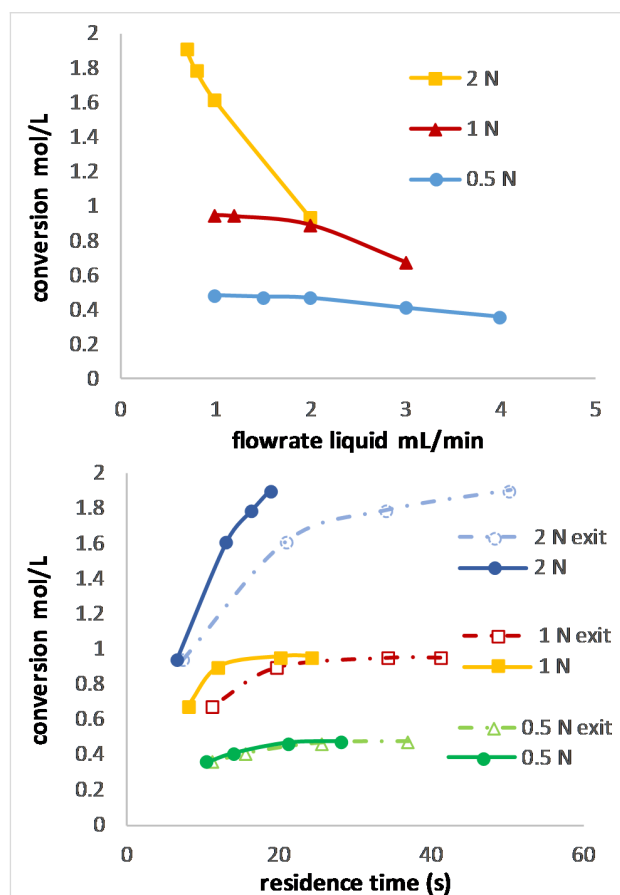


Figure 12: Absolute conversion of various concentrations of alpha-terpinene at 407 nm using 0.32 mmol/L of TPP (H) as a function of the liquid flow rate (top) and the residence time (bottom).

the reaction mixture was also not considered, but for pure toluene, it would be 14% (0.5 N) or 4% (2 N) less gas volume [40]. Furthermore, the gas-to-liquid ratio change with the modification of the alpha-terpinene concentration impacts the flow

pattern (droplet/bubble size), which could, in turn, have an impact on the conversion [41]. But the main limitation was the light itself, as can be seen in Figure 11. About the same absolute conversion was obtained for similar liquid flow rates independent from the residence time.

Conclusion

We developed a reliable, quick, and simple approach to find the appropriate starting concentration of a photocatalyst for a photooxidation reaction in a flow reactor. This was achieved by linking the catalyst concentration to the channel height of the flow reactor and to the emission spectrum of the light source, using the Bouguer–Lambert–Beer law. Since the conditions applied were outside of, but close to the range of this law, the determined concentrations will be close to, but not exactly the optimum. The approach was tested with different light sources, and it was shown that it is important to match the LED to the reaction absorption spectrum. This is important as a variation of only a few nm can have a big impact on the catalyst concentration needed. We believe that this methodology will help in choosing the right catalyst and the right wavelength to eliminate scale-up issues encountered during the industrialization of photooxidation reactions.

Supporting Information

Supporting Information File 1

Descriptions of material and methods, flow setup, and LED characterization.

[<https://www.beilstein-journals.org/bjoc/content/supplementary/1860-5397-16-78-S1.pdf>]

Acknowledgements

We would like to thank Dr. Jürgen Kolz from Magritek for his support with NMR analytics and Dr. Edward “Ed” J Fewkes for his help with the manuscript and scientific discussions.

ORCID® iDs

Clemens R. Horn - <https://orcid.org/0000-0002-8105-6932>

Sylvain Gremetz - <https://orcid.org/0000-0001-9851-0604>

References

1. Politano, F.; Oksdath-Mansilla, G. *Org. Process Res. Dev.* **2018**, *22*, 1045–1062. doi:10.1021/acs.oprd.8b00213
2. Cambié, D.; Bottecchia, C.; Straathof, N. J. W.; Hessel, V.; Noël, T. *Chem. Rev.* **2016**, *116*, 10276–10341. doi:10.1021/acs.chemrev.5b00707
3. Beeler, A. B. *Chem. Rev.* **2016**, *116*, 9629–9630. doi:10.1021/acs.chemrev.6b00378
4. Garlets, Z. J.; Nguyen, J. D.; Stephenson, C. R. J. *Isr. J. Chem.* **2014**, *54*, 351–360. doi:10.1002/ijch.201300136
5. Knowles, J. P.; Elliott, L. D.; Booker-Milburn, K. I. *Beilstein J. Org. Chem.* **2012**, *8*, 2025–2052. doi:10.3762/bjoc.8.229
6. Noël, T. *J. Flow Chem.* **2017**, *7*, 87–93. doi:10.1556/1846.2017.00022
7. Di Filippo, M.; Bracken, C.; Baumann, M. *Molecules* **2020**, *25*, 356. doi:10.3390/molecules25020356
8. Pfoertner, K.-H.; Oppenländer, T. Photochemistry. *Ullmann's Encyclopedia of Industrial Chemistry*; Wiley-VCH: Weinheim, Germany, 2012. doi:10.1002/14356007.a19_573.pub2
9. Berton, M.; de Souza, J. M.; Abdiaj, I.; McQuade, D. T.; Snead, D. R. *J. Flow Chem.* **2020**, *10*, 73–92. doi:10.1007/s41981-019-00060-x
10. Lavric, E. D.; Woehl, P. *Chim. Oggi* **2009**, *27* (3), 45–48.
11. Woitalka, A.; Kuhn, S.; Jensen, K. F. *Chem. Eng. Sci.* **2014**, *116*, 1–8. doi:10.1016/j.ces.2014.04.036
12. Hone, C. A.; Roberge, D. M.; Kappe, C. O. *ChemSusChem* **2017**, *10*, 32–41. doi:10.1002/cssc.201601321
13. Nieves-Remacha, M. J.; Kulkarni, A. A.; Jensen, K. F. *Ind. Eng. Chem. Res.* **2013**, *52*, 8996–9010. doi:10.1021/ie4011707
14. Gemoets, H. P. L.; Su, Y.; Shang, M.; Hessel, V.; Luque, R.; Noël, T. *Chem. Soc. Rev.* **2016**, *45*, 83–117. doi:10.1039/c5cs00447k
15. Schenck, G. O. Light sources and light filters in preparative organic photochemistry. In *Preparative Organic Photochemistry*; Schönberg, A., Ed.; Springer: Berlin, Germany, 1968; pp 472–494. doi:10.1007/978-3-642-87918-0_46
16. Sender, M.; Ziegenbalg, D. *Chem. Ing. Tech.* **2017**, *89*, 1159–1173. doi:10.1002/cite.201600191
17. Ghazali, S. K.; Azim, F. S. S.; Adrus, N.; Jamaluddin, J. *J. Photopolym. Sci. Technol.* **2019**, *32*, 705–710. doi:10.2494/photopolymer.32.705
18. Cho, J.; Park, J. H.; Kim, J. K.; Schubert, E. F. *Laser Photonics Rev.* **2017**, *11*, 1600147. doi:10.1002/lpor.201600147
19. Fewkes, E. J.; Horn, C. R.; Logunov, S. L. Flow reactor for photochemical reaction. U.S. Patent US10,258,957, March 26, 2015. We have already used successfully LED at 300 nm, but the power of the LEDs is low (40 mW) and long residence times are required to obtain conversion.
20. Bonfield, H. E.; Knauber, T.; Lévesque, F.; Moschetta, E. G.; Susanne, F.; Edwards, L. J. *Nat. Commun.* **2020**, *11*, 804. doi:10.1038/s41467-019-13988-4
21. Yueh, H.; Gao, Q.; Porco, J. A., Jr.; Beeler, A. B. *Bioorg. Med. Chem.* **2017**, *25*, 6197–6202. doi:10.1016/j.bmc.2017.06.010
22. Gauron, G.; Ao, J.; Gremetz, S.; Horn, C. R. *Chim. Oggi* **2018**, *36* (4), 12–16.
23. Lévesque, F.; Seeberger, P. H. *Org. Lett.* **2011**, *13*, 5008–5011. doi:10.1021/ol2017643
24. Hunter, R.; Josland, S.; Moore, J.; Guthrie, D.; Robertson, M. J.; Oelgemöller, M. *Curr. Org. Chem.* **2018**, *22*, 2501–2508. doi:10.2174/1385272822666181109103342
25. Radjagobalou, R.; Blanco, J.-F.; Dechy-Cabaret, O.; Oelgemöller, M.; Loubière, K. *Chem. Eng. Process.* **2018**, *130*, 214–228. doi:10.1016/j.cep.2018.05.015
26. Hamami, Z. E.; Vanoye, L.; Fongarland, P.; de Bellefon, C.; Favre-Régouillon, A. *ChemPhotoChem* **2019**, *3*, 122–128. doi:10.1002/cptc.201800201
27. Bunsen, R.; Roscoe, H. *Ann. Phys. (Berlin, Ger.)* **1857**, *176*, 43–88. doi:10.1002/andp.18571760104
28. Bunsen, R.; Roscoe, H. *Ann. Phys. (Berlin, Ger.)* **1857**, *176*, 481–516. doi:10.1002/andp.18571760402

29. Bunsen, R.; Roscoe, H. *Ann. Phys. (Berlin, Ger.)* **1857**, *177*, 235–263. doi:10.1002/andp.18571770605
30. Mäntele, W.; Deniz, E. *Spectrochim. Acta, Part A* **2017**, *173*, 965–968. doi:10.1016/j.saa.2016.09.037
31. Mayerhöfer, T. G.; Mutschke, H.; Popp, J. *ChemPhysChem* **2016**, *17*, 1948–1955. doi:10.1002/cphc.201600114
32. Sambiagio, C.; Noël, T. *Trends Chem.* **2020**, *2*, 92–106. doi:10.1016/j.trechm.2019.09.003
33. Tolbin, A. Y.; Pushkarev, V. E.; Tomilova, L. G.; Zefirov, N. S. *Phys. Chem. Chem. Phys.* **2017**, *19*, 12953–12958. doi:10.1039/c7cp01514c
34. Ito, M. *J. Mol. Spectrosc.* **1960**, *4*, 106–124. doi:10.1016/0022-2852(60)90072-2
35. Taniguchi, M.; Lindsey, J. S. *Photochem. Photobiol.* **2018**, *94*, 290–327. doi:10.1111/php.12860
36. Fukuzumi, S.; Yuasa, J.; Miyagawa, T.; Suenobu, T. *J. Phys. Chem. A* **2005**, *109*, 3174–3181. doi:10.1021/jp050347u
37. Salker, A. V.; Gokakakar, S. D. *Int. J. Phys. Sci.* **2009**, *4* (6), 377–384.
38. Sharghi, H.; HassaniNejad, A. *Tetrahedron* **2004**, *60*, 1863–1868. doi:10.1016/j.tet.2003.12.030
39. Ludvíková, L.; Friš, P.; Heger, D.; Šebej, P.; Wirz, J.; Klán, P. *Phys. Chem. Chem. Phys.* **2016**, *18*, 16266–16273. doi:10.1039/c6cp01710j
40. Wu, X.; Deng, Z.; Yan, J.; Zhang, Z.; Zhang, F.; Zhang, Z. *Ind. Eng. Chem. Res.* **2014**, *53*, 9932–9937. doi:10.1021/ie5014772
41. Nakano, M.; Morimoto, T.; Noguchi, J.; Tanimoto, H.; Mori, H.; Tokumoto, S.-i.; Koishi, H.; Nishiyama, Y.; Kakiuchi, K. *Bull. Chem. Soc. Jpn.* **2019**, *92*, 1467–1473. doi:10.1246/bcsj.20190117

License and Terms

This is an Open Access article under the terms of the Creative Commons Attribution License (<http://creativecommons.org/licenses/by/4.0>). Please note that the reuse, redistribution and reproduction in particular requires that the authors and source are credited.

The license is subject to the *Beilstein Journal of Organic Chemistry* terms and conditions: (<https://www.beilstein-journals.org/bjoc>)

The definitive version of this article is the electronic one which can be found at: doi:10.3762/bjoc.16.78